

Design and Evaluation of an Energy Storage System for Helicopters

C Klumpner, M Rashed

*The University of Nottingham, UK
klumpner@ieee.org*

Keywords: battery, EMI filter, energy storage system, interleaved converter, supercapacitors.

Abstract

This paper presents the design and evaluation of an energy storage system (ESS) for helicopters with the aim to recover the kinetic energy in the rotor available after landing and to be able to control the 270V dc bus voltage during load disturbances. A study is conducted in order to identify the suitable mix of commercially available energy storage devices with the aim of obtaining the minimum weight, exploring also the possibility to implement a hybrid supercapacitor-battery system. On the converter side, commercially available Silicon and Silicon-Carbide devices have been evaluated to achieve also the smallest size/weight.

1 Introduction

The “more electric aircraft” [1] is a concept that aims at employing more electrical technologies in the operation of aircrafts with the purpose of minimizing the overall weight of the systems and increasing the efficiency of energy conversion (electrical motors are significantly more efficient than hydraulic) that would ultimately reduce the fuel consumption and associated costs. Using more energy storage in the form of electrochemical energy storage devices such as supercapacitors and batteries is part of this concept with the aim of handling the power peak requirements so that the generators can be sized based on the average and not peak power requirement, whilst the availability of storing regenerated power from flying surfaces or propellers that is temporarily available, may further reduce fuel consumption.

This paper investigates the design of an energy storage system (ESS) that would enable the recovery of regenerative power that can be extracted from the kinetic energy of the main propeller of a helicopter immediately a successful landing. This energy can be used also to provide an engine start without any assistance from a ground power unit which may be a very likely situation in remote locations.

2 Optimising the Energy Storage Size

In order to optimise the implementation of the energy storage system, the power and energy requirements need to be first analysed. In this project, there are three requirements [2]:

- Be able to provide emergency power for a given duration to power essential avionics, in case of a generator failure;

- Be able to capture the full kinetic energy available from the main rotor blades following a custom power profile as shown in Fig. 1. This consist of a very high peak regenerative power as available at the beginning of the rotor braking process mainly due to the high rotational speed. This needs to be very high and will decay very fast (seconds) to make sure only a small amount of the kinetic energy is lost by causing unnecessary air turbulence;
- Be able to reuse the recovered energy during braking to perform a successions of engine starts;

Three options are available to implement the ESS functions:

A) Implement a battery only system. The initial size is based on the emergency power requirements but then the peak charging power requirement is analysed in relation to the charging current capability of the battery. Since most batteries will have a highly asymmetric charge vs discharge current/power capability, it is important that both the charging and the discharging requirement are separately assessed. Even though Li-ion batteries have currently the highest specific energy and power, two types of secondary battery exist:

- i) energy cells (EC) such as Lithium Cobalt oxide, similar to the cells used in laptops and mobile phones that have the highest specific energy (>240Wh/kg) but a limited charging and discharging current ($I_{ch}=0.5-2C$; $I_{disch}=1-5C$). It should be noted that the significantly low charging current is the limiting factor in this application.
- ii) power cells (PC) such as the Lithium-Iron-phosphate-oxide (LiFePO4) similar to the ones used in cordless power tools, which have lower cell voltage (3.2V) but can handle higher current/power ($I_{ch}=2-5C$; $I_{disch}=10-20C$).

B) Implement a supercapacitor only ESS where the minimum supercapacitor size is determined based on the energy corresponding for the emergency power requirement and due to the symmetry of the device when charging/discharging, this will result in the highest power peak value needed during charging or discharging. The operation assumes that the supercapacitor is initially charged at a voltage V_{mean} that corresponds to the mid energy range that would allow for the device to be charged or discharged with the maximum energy level required by the application W_{regen} without exceeding the maximum or minimum device voltage V_{max} and V_{min} .

$$W_{regen} = 0.5(W_{max} - W_{min}) = 0.5C(V_{max}^2 - V_{min}^2) \quad (1)$$

$$V_{mean}/V_{max} = \sqrt{0.5(1 + V_{min}/V_{max})} \quad (2)$$

It should be noted that an optimal minimum device voltage V_{min} needs to be chosen when designing a supercapacitor energy storage system and a trade-off between maximising

the device utilisation which is the maximum energy that can be extracted ($W_{\max} - W_{\min}$) relative to the device rated energy (W_{\max}) and lowering the maximum current rating of the converter that controls the supercap power flow $I_{\max} = P/V_{\min}$. Different technologies exist that can maximize the current/power capability such as the EDLC technology, whilst the pseudocapacitors or the hybrid supercapacitors provide upto twice higher specific energy (Wh/kg) but significantly smaller power peak handling capability.

C) Implement a hybrid battery-supercapacitor system where the supercapacitors are handling most of the regenerative power peak requirement whilst the battery which is there to provide the emergency power requirement, can also absorb some power (P_{bat}) during the time the ESS is supposed to absorb the braking power peaks. Fig. 1 illustrates this concept by highlighting the regenerative power profile that has to be handled by the ESS and which part of the power is handled by the supercaps and the battery. If after landing the helicopter will rest for a longer period of time, it is possible for the energy stored in the supercaps to be moved into the battery immediately after the incoming braking power decreases below P_{bat} . If the helicopter is supposed to take off soon after landing, it may be more efficient to keep some of the recovered energy in the supercap in case an engine start that requires significant power ($P > P_{\text{bat}}$), is needed.

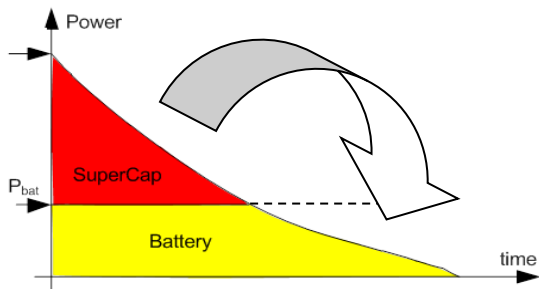


Fig. 1. Handling of a power peak requirement by a hybrid energy storage system during the rotor braking.

2.1 Comparing the performance of different supercapacitor technologies

There are several factors that need to be considered when choosing which device should be used when designing a supercapacitor based ESS. Some of the performance (rated capacitance and voltage range of available cells, internal resistance, geometrical dimensions and weight, maximum current, specific power and energy) can be assessed by analysing the datasheets which allow users to determine which cell can be used to build a stack of an optimum voltage and then determine how the project requirements/stresses relate to the cell level and if the particular cell can cope with it. An interesting example of how the datasheet parameters needs to be interpreted when evaluating the actual specific energy capability of a device is related to the device voltage range. Lithium based supercapacitors are supposed to offer a significantly higher energy density mainly due to the higher maximum operating voltage which is 3.8V compared to 2.7-2.85V for EDLC supercaps or 2.3V for pseudocapacitors and hybrid supercaps. This in theory should increase the specific energy by a factor of $(3.8/2.7)^2=2$ solely due to the higher

operating voltage. If however, the minimum voltage is considered (2.2V for Lithium supercaps), based on Equation (1), this means that only 66.5% of the rated energy can be used compared to a significantly higher utilisation level for the other technologies. The advantage is that a higher minimum device voltage means that a converter built to process a given power level, would require smaller current ratings which may result in lower converter weight.

A more in-depth analysis can be performed by testing a restricted number of preselected supercapacitor samples. In this project, several devices were characterised and their equivalent series resistance and equivalent capacitance versus frequency was recorded for different bias voltage which is representative for their operating voltage range and these are shown in Fig. 2. This evaluation reveals two important aspects. The first is the variation of the internal resistance of the device which affects the capability of the device to deliver the required power with the change in bias voltage of the device, which was observed with most supercapacitor devices that were tested. The variation of the equivalent series resistance of four devices is shown in Fig. 2a at both minimum and maximum voltage. It can be seen that some devices (the pseudocap from Nesscap [3] and the hybrid supercap from Ioxus [4]) show higher resistance at low voltage which will further degrade the specific power whilst the ELDC from both Maxwell [5] and Ioxus show lower resistance at lower voltage.

The last aspect to be considered is the variation of the capacitance with the bias voltage (Fig. 2b). As explained in the beginning of this section, an ESS based on supercaps that is designed to be able to deliver/absorb a given amount of energy as defined in the specification, at any given moment, needs to be designed to operate at a “mid energy” operating point as defined by Equation (2), which assumes that the capacitance is constant with the bias voltage. It can be noted that some devices experience an increase of capacitance with the bias voltage, which is beneficial for the application. As

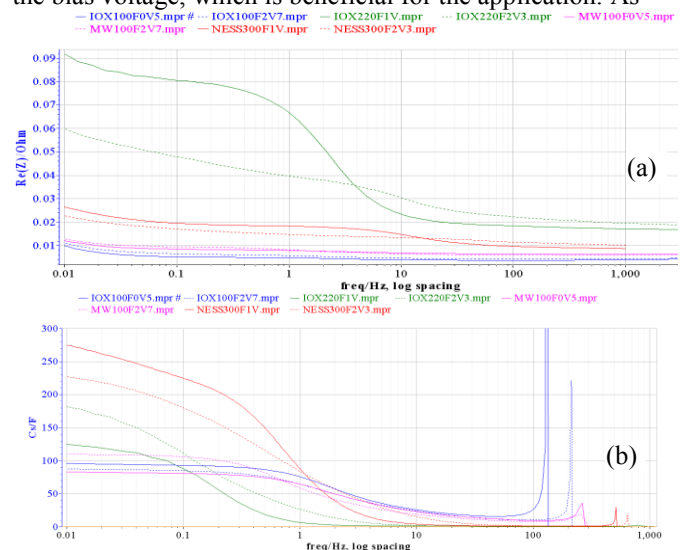


Fig. 2. Variation of a) the equivalent series resistance and b) the capacitance vs frequency at minimum and maximum operating voltage for different devices: 100F EDLC (Ioxus), 220F hybrid (Ioxus) 300F (Nesscap) 100F EDLC (Maxwell).

the device charges, its capacitance increases and this means it can store even more electrical charge for a given voltage increment. However, other devices exhibit a decrease in capacitance with voltage increase which is less beneficial, resulting in a need to oversize the required capacitance.

An interesting behaviour has been noted with the 1.1kF Lithium supercap [6], which exhibits a significant decrease of the low frequency capacitance as shown in Fig. 3, from 1.15kF @2.2V bias down to 900F@3V bias (almost -20% of the rated value), followed by an increase to almost 1.3kF @3.8V bias. Whilst exploitation of the device above 3.2V may be very beneficial for the application, it can be noted that in order to guarantee that sufficient energy is available when discharging from V_{mean} as defined in Equation (2) to V_{min} , oversizing the device may be needed as explained earlier.

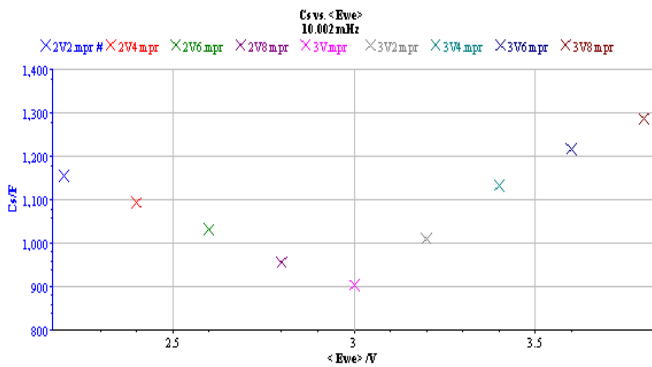


Fig. 3: Variation of the low frequency (10mHz) capacitance with the bias voltage for a 1.1kF Lithium based supercap.

2.2 Sizing the hybrid ESS with energy dense battery cells

Same options exist when considering a hybrid ESS. Use an EC or a PC for the battery stack to provide the full emergency power requirement that will result in less mass for EB or more mass for PB whilst assisting the handling of the regenerative power peak with less power for EC or more power for PB. This situation is illustrated in Fig. 4 where the size of a hybrid system consisting of EC battery and different types of supercaps is calculated. Note that the devices chosen are representative for the technology of commercial devices available in year 2013. The variation of the total mass of the battery and supercap cells as a result of oversizing the battery to be able to provide more of the regen power peak is shown in Fig. 4 for two different supercap technologies from the same manufacturer (IOXUS): the 100F/2.7V EDLC and the 820F/2.3V hybrid device. It can be seen that when using EC for the battery, the minimum weight of the energy storage cells is always achieved when the battery using EC is the smallest as defined by the emergency power requirements and that the hybrid supercap device offers the lowest overall weight for the ESS cells.

Table 1 summarises the weight of the energy storage cells in a hybrid system consisting of Lithium cobalt oxide energy cells and a choice of six supercapacitor devices that were identified in a technology survey in year 2013. It can be seen that the smallest ESS weight of cells of 26.8kg is achieved by using the 1.1kF Lithium ion supercapacitors from JSR followed by the use of hybrid supercap devices produced by Ioxus and

Yunasko [7] (34.5-35.6kg) whilst the most power dense supercap technology (ELDC) result in weights of ESS cells in excess of 45kg.

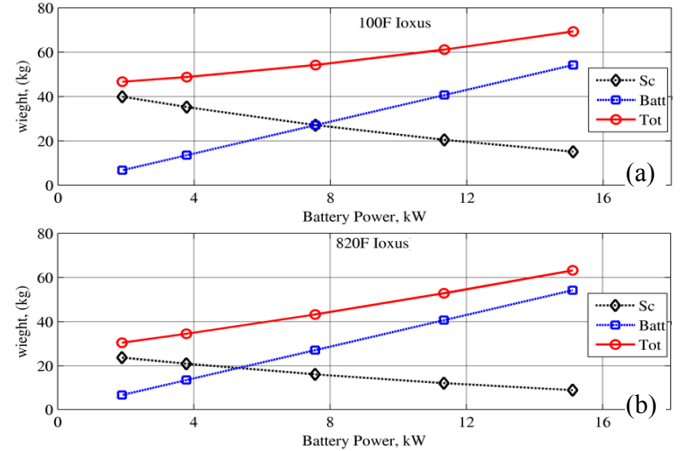


Fig.4: Illustrating how the weight of the energy storage cells changes as a function of how much power the EC battery handles for different supercapacitor devices.

Supercap device	Weight of ESS cells
100F/2.7V (Ioxus)	48.8kg
2000F/2.7V(Nesscap)	47.9kg
2000F/2.7V (Maxwell)	45.2kg
820F/2.3V (Ioxus)	34.5kg
480F (Yunasko)	35.6kg
1.1kF/3.8V Lithium (JSR)	26.8kg

Table 1: Summary of the ESS cell weight calculation when EC are used with a variety of supercap devices

2.3 Sizing the hybrid ESS with power dense battery cells

In the previous approach, it has been noted that oversizing the EC battery to increase the EC battery power contribution to the peak braking power handling cannot provide weight reductions due to poor power density of the EC. For this reason, another approach when implementing the hybrid arrangement is to use a PC battery that can enable significantly faster charging such as Lithium-Iron-Phosphate (LiFePO₄ or also referred as LPO) or based in Lithium-Titanate (Li₂-Ti-O₃ or LTO) from Altairnano [8]. Whilst the LPO is a widely available technology used in power tools and electric vehicles, the LTO device is not very widely available, with very few cell sizes commercially available. This means that even though the chemistry may offer a great implementation potential, due to the lack of a well matched cell size that could provide a well matched stack voltage with the application and capacity/maximum charging power, the result will be a suboptimal system. This can be seen in Table 2 where the 65 series connected 8Ah LPO cells needed to provide the emergency power requirement offer a more convenient stack voltage level (208V) for interfacing directly to a 270V bus compared to the 124V for the LTO cells.

The exercise can be extended to estimate the weight of a battery only ESS implementation and it becomes clear that whilst the weight of the LPO system is prohibitive (105kg), the LTO implementation is competitive (29.2kg).

	LPO	LTO
Cell voltage	3.2 V	2.26V
Cell capacity	8Ah	13Ah
Weight of cell	0.3kg	0.4kg
Specific Energy	85Wh/kg	75.7Wh/kg
Spec charging Power	427W/kg	757W/kg
i) Battery stack to supply for emergency power		
No cells series/parallel	65Sx1P	55Sx1P
Stack weight	19.5kg	22kg
Peak charging power	8.4kW (5C)	16.9kW(10C) 33.8kW(20C)
Stack voltage	208V	124V
ii) Battery only ESS design for full braking power		
No cells series/parallel	70Sx5P	73Sx1P(20C)
Stack weight	105kg	29.2kg
Stack voltage	224V	169V

Table 2: Summary of the power dense battery cell implementations available when the stack is designed to provide storage of i) the energy for emergency situation and ii) the full braking power (battery only).

Calculations of the overall weight of the cells of a hybrid ESS system using power battery cells show that the best combination will involve the same 1.1kF Lithium supercapacitor resulting in a total weight of 29.1kg with LPO cells and 26.9kg when the LTO cells are used, which is very close to the minimum weight of 26.8kg achieved when using energy battery cells and the 1.1kF Lithium supercapacitor.

Considering however that the hybrid ESS system would require two separate power converters and considering that the LTO only implementation is only 2.3kg heavier, it was decided to choose the battery only implementation and using 75 cells that can be arranged in 5 modules of 15 cells each and Fig. 5 shows the physical implementation of the battery stack consisting of five modules. On top of each module, the battery monitoring electronic units recommended by the cell manufacturer are mounted and interconnected via serial communication, which can be connected to as supervisory control, enabling the monitoring of individual cell voltages, temperatures and string voltage and currents.



Fig. 5: Implementation of the battery stack consisting of 5 modules with 15 Altairnano 13Ah cells each.

3 Design of the power converter

Fig. 6 shows the topology of a 2-channel interleaved DC/DC converter consisting of two half-bridge inverter legs that has been chosen to interface the battery stack to the 270V dc-bus. Even though initially, a solution with coupled inductors has been considered, which is known to enable significant reduction in the core size, a solution based on independent/non-coupled magnetics has been chosen for the following reasons: (i) coupled magnetics result in small leakage inductance which opposes the common mode output current. In applications where the load is highly capacitive as is the case of a battery system, this will result in significant switching current ripple that would require the addition of an additional inductor; (ii) the converter has a very important role in maintaining the regulation of the 270V bus voltage during significant dc-bus disturbance and for this reason, it is desired that in case of a fault/failure of one converter channel, the other channel to be able to operate at full current capability, and this would not have been possible in case the two channels are magnetically coupled.

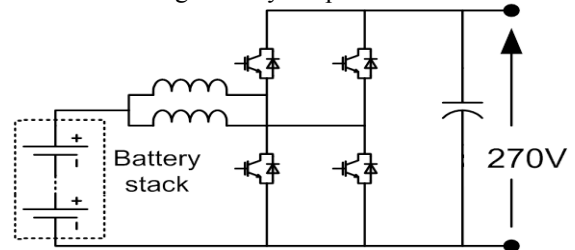


Fig. 6: The 2-channel interleaved DC/DC converter topology chosen to interface the battery stack to the 270V bus

Following the choice of the converter topology, a study to estimate the power density of the converter depending on the technology of switches available (note this study has been carried out in 2014), has been carried out. Two power modules have been identified: the last generation silicon Infineon IGBT 600V/75A [9] in a low weight Econopak package operating at 20kHz versus the first generation Cree 1.2kV/100A SiC MOSFET [10] using a fairly bulky/standard power module packaging that embeds a single half bridge, but operating at 40kHz. First, an analytical model to determine the variation of switching ripple versus duty cycle has been determined in order to identify the worst case operating points which would then be used in sizing the inductance needed by the two converters. Fig. 7 shows the current ripple vs duty cycle characteristic typical for a 4-channel interleaved DC/DC converter required in the Si implementation (due to reduced current capability). The stresses in the key operating points can then be validated by simulation (not shown). This approach enabled the choice of the inductance needed for both converters and to identify the current stresses (peak current which is relevant for the choice of the switches and the airgap of the inductors to avoid saturation and current ripple in inductors) which was later used to design the inductors (selecting the core geometry, calculate no. of turns etc) which then can be used in estimating the weight of the magnetics and the losses.

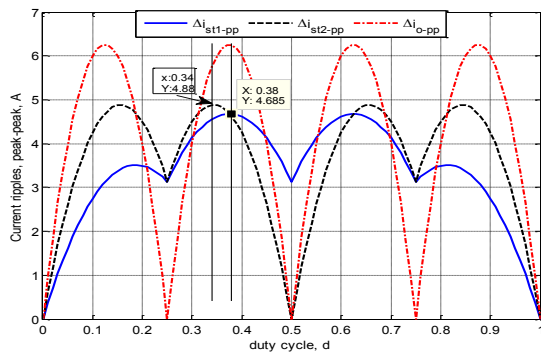


Fig. 7: Peak-peak channel current ripples for the various stages at different duty cycles.

The PSIM simulation model was also used to determine the semiconductor power losses of both converter implementations in the key operating points (maximum current) to estimate the size/weight of the heatsink (air cooling was assumed). This enabled the estimation of the total converter loss and weight and are summarised in Table 3.

	15kW/20 kHz Silicon IGBT, Infineon	22.5kW/40 kHz SiC MOSFET, Cree
Loss Magnetics	109.2 W	170.8
Semiconductor W	320.2	376.6
Total losses, W	429.4	547.4
Losses in %	2.86 %	2.43 %
Heatsink ΔT_{h-a}	20K	41.8K
R_{th-h-a} of heatsink	0.0625 K/W	0.111 K/W
Mass of heatsink	2.13 kg	1.2 kg
Mass of magnetics	3.16 kg	3.14kg
Power module mass	0.048kg	0.8kg
Electronics, g	0.3kg	0.3kg
Total weight, g	5.37kg	5.44kg
Specific power	2.78kW/kg	4.17kW/kg

Table 3: Comparison of the power losses, weight and power integration potential of silicon versus SiC power modules

It could be noticed that due to the need to minimise weight, both converters will operate with a similar level of losses (2.4-2.9%) and although the commercially available SiC power module is clearly not optimised for high power density (18 times heavier than the Infineon package), the system implementation provides 50% more specific power (kW/kg) than the silicon due to the weight savings in the inductor (size is similar but SiC provides 50% more power) and smaller heatsink, as the SiC module can work with 20K higher device temperature. This is the reason why the choice was made to implement the power stage using SiC power modules.

4 Experimental evaluation of the ESS

Fig. 8a shows the schematic of the actual implementation of the energy storage system, including the battery stack formed of five 15 cell LTO modules, the inrush circuit, the interleaved DC/DC converter, the EMC filter and the

associated switchgear and overcurrent protections that are needed to provide safe operation of the system. Fig. 8b shows the actual implementation of the power converter (BDCR box in Fig. 8a). The EMC filter has been designed to maintain the resulting DC-link voltage ripple below the limits specified in the power quality standards of DO160. This ripple is caused by the switching current ripple having the most significant harmonic at twice the switching frequency. The amplitude of this current ripple as percentage of the DC current is dependent on the modulation index (which is the ratio between battery stack voltage and actual 270V bus voltage) whilst the DC current is dependent on the power reference (therefore dependant also on the battery stack voltage).

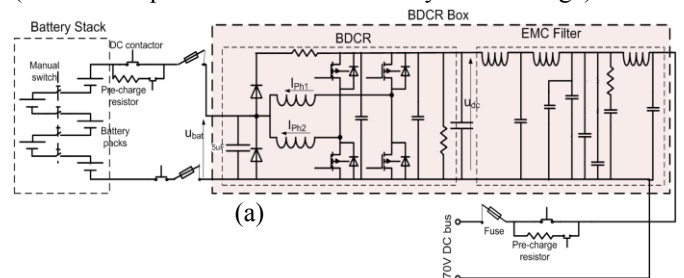


Fig. 8: a) Schematic of the battery energy storage system; b) Actual implementation of the converter (BDCR box).

Fig. 9 shows the voltage ripple seen on the 270V bus in frequency domain in relation to the allowed voltage ripple limits and is clear that the 80 kHz voltage ripple is very close to the allowed limit. The shape of the allowed ripple envelope also shows that very fast switching converters cannot really benefit from fast switching since above 50 kHz, the allowed harmonic limit by the power quality standard decreases very abruptly with the increase in frequency which means a bulkier/heavier filter may be needed (note that the weight of the EMC filter has not been considered in the estimation of the power density given in the previous section – Table 3). The testing of the power converter has been done in an arrangement involving two identical power converters connected in parallel that circulate the electrical power and having a DC power supply set at 200V connected to the low voltage side (battery port) to supply the system losses.

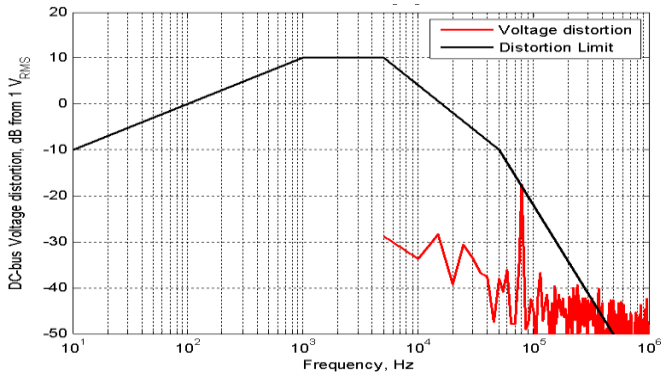


Fig.9: The resulting DC-bus voltage harmonic spectrum in relation to the DO160 limits for 15kW operation

Fig. 10 shows the converter efficiency versus loading and the measured temperature of the heatsink. The efficiency level is significantly better than predicted in Table 3 due to higher battery port voltage (200V) and lower current.

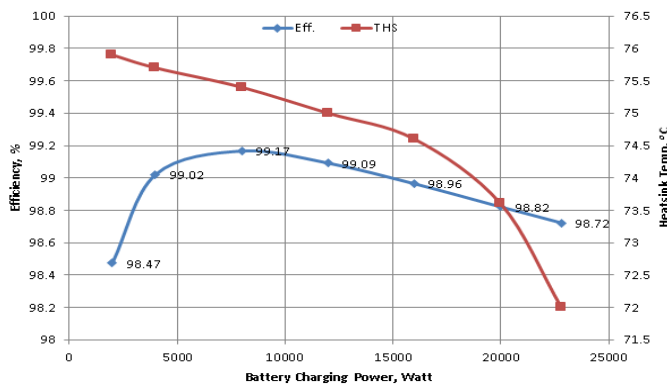


Fig. 10: Efficiency of the main converter and heatsink temperature in charging mode of operation.

The transient response of the DC-DC converter as result of processing the braking power profile as imposed in the project specification is shown in Fig. 11. These tests were used to validate the capability of the converter to process the peak power/current from cooling point of view. It should be noted that the frequency of the switching ripples seen in the current is affected by aliasing due to slow sampling required to capture the full test (50s).

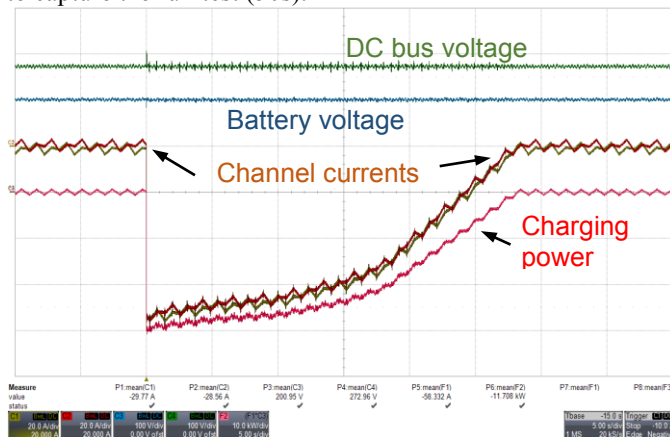


Fig.11: Experimental result of the battery converter processing the specified braking power profile.

In order to evaluate the true high speed dynamic response, the setup consisting of the two identical converters independently controlled, that are circulating power between the DC bus and the battery port is subject to a transient of 28kW power step injected in the 270V DC-bus by the auxiliary converter. Fig. 12 shows the fast response of the control of the main converter where the DC-bus voltage experiences an overshoot of less than 7V ($V_{bus\ pk}=276.9V$).

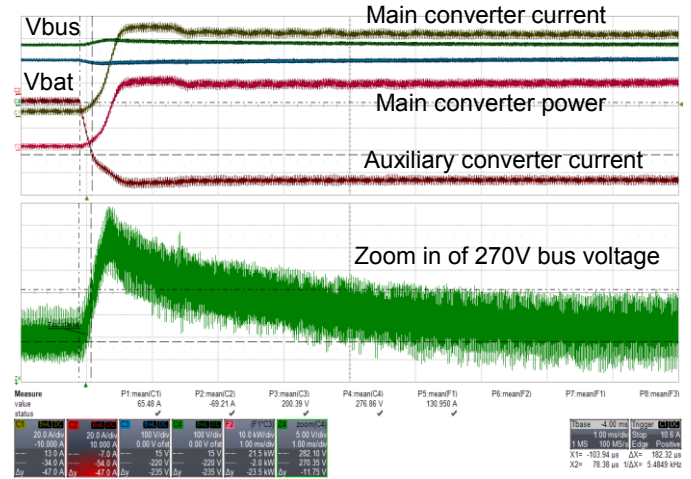


Fig. 12: DC bus voltage control dynamic response to sudden application of a 28kW braking power step.

5 Conclusions

This paper presents the design and evaluation of an energy storage system suitable for helicopters. This included the selection of the energy storage devices in order to minimize overall weight of the system, the design and implementation of the power converter based on the stresses experienced in the most challenging operating point and the experimental evaluation of the system performance.

Acknowledgements

The research leading to these results has received funding from the European Union's Seventh Framework Programme (FP7/2007-2013) for the Clean Sky Joint Technology Initiative under grant agreement n° CS-GA-GRC-2011-03-308129 (project “Multi-source regenerative system power conversion – REGENSYS).

References

- [1] www.moreelectricaircraft.com
- [2] Clean Sky Joint Undertaking – JTI-CS-2011-5-GRC-03-11 – Multi-source regenerative systems power conversion - Topic description, pp. 85-92.
- [3] Nesscap – Supercapacitors catalogue – online.
- [4] IOXUS – Supercapacitor catalogue – online.
- [5] Maxwell - Ultracapacitor catalogue – online.
- [6] JSR –1100F Ultimo Lithium supercapacitor datasheet.
- [7] Yunasko - Supercapacitor catalogue – online.
- [8] Altainano – Datasheet 13Ah Lithium Titanate cell– online
- [9] Infineon – F4-75R06W1E3 Econopak module datasheet
- [10] Cree –1.2kV/100A SiC half bridge module datasheet